Proc. Natl. Acad. Sci. USA
Vol. 93, pp. 6731–6736, June 1996
Pharmacology

Characterization of a murine *Ahr* null allele: Involvement of the Ah receptor in hepatic growth and development

(dioxin/2,3,7,8-tetrachlorodibenzo-*p*-dioxin/gene targeting/liver)

JENNIFER V. SCHMIDT*, GLORIA HUEI-TING SU†‡, JANARDAN K. REDDY§, M. CELESTE SIMON‡, AND CHRISTOPHER A. BRADFIELD*¶

Departments of Molecular Pharmacology and Biological Chemistry and §Pathology, Northwestern University Medical School, Chicago, IL 60611; and †Committee on Immunology and ‡Department of Medicine and Howard Hughes Medical Institute, The University of Chicago, Chicago, IL 60637

Communicated by James A. Miller, University of Wisconsin, Madison, WI, March 5, 1996 (received for review December 12, 1995)

ABSTRACT **The Ah receptor (AHR) is a ligand-activated transcription factor that mediates a pleiotropic response to environmental contaminants such as benzo[a]pyrene and 2,3,7,8-tetrachlorodibenzo-*p*-dioxin. In an effort to gain insight into the physiological role of the AHR and to develop models useful in risk assessment, gene targeting was used to inactivate the murine *Ahr* gene by homologous recombination. *Ahr*$^{-/-}$ mice are viable and fertile but show a spectrum of hepatic defects that indicate a role for the AHR in normal liver growth and development. The *Ahr*$^{-/-}$ phenotype is most severe between 0–3 weeks of age and involves slowed early growth and hepatic defects, including reduced liver weight, transient microvesicular fatty metamorphosis, prolonged extramedullary hematopoiesis, and portal hypercellularity with thickening and fibrosis.**

The Ah receptor (AHR) is a ligand-activated transcription factor that regulates a biphasic pleiotropic response to a variety of structurally related environmental contaminants (1, 2). Upon binding polycyclic aromatic hydrocarbons (PAHs), such as benzo[a]pyrene, the AHR increases the expression of xenobiotic metabolizing enzymes, including the cytochrome P450IA1, P450IA2 and P450IB1-dependent monooxygenases, the glutathione *S*-transferase Ya subunit, quinone oxidoreductase, and UDP-glucuronosyltransferase (3–8). In response to more potent halogenated aromatic agonists like 2,3,7,8-tetrachlorodibenzo-*p*-dioxin (TCDD), the AHR induces xenobiotic metabolism and also mediates a spectrum of toxic responses, including thymic involution, teratogenesis, tumor promotion, wasting, and epithelial hyperplasia and metaplasia (9–11).

The AHR is a member of a family of transcription factors containing basic/helix–loop–helix and PAS homology domains (bHLH–PAS) (1). In response to agonist binding within the PAS domain, the cytosolic AHR undergoes a conformational change, translocates to the nucleus, dissociates from the 90-kDa heat shock protein, and dimerizes with a second bHLH–PAS protein known as the Ah receptor nuclear translocator (ARNT) (12–16). This heterodimer interacts with dioxin-responsive enhancer elements upstream of target genes and activates their transcription. Despite our mechanistic understanding of the role of the AHR in regulating xenobiotic metabolism, we still have little understanding of how the AHR mediates the toxic responses of halogenated agonists and why such responses are produced only by high affinity, poorly metabolized ligands such as TCDD.

To examine the importance of the AHR in normal vertebrate biology, we have used gene targeting to create mice with a mutation at the *Ahr* locus. We anticipated that such a mutant could provide insights into additional physiological roles of the AHR and would represent a powerful model to understand the toxicology of halogenated aromatic pollutants like TCDD.

The publication costs of this article were defrayed in part by page charge payment. This article must therefore be hereby marked "*advertisement*" in accordance with 18 U.S.C. §1734 solely to indicate this fact.

MATERIALS AND METHODS

Construction of the *Ahr* Targeting Vector. Three P1 clones were isolated from a 129/Sv mouse genomic library by using a PCR approach (Genome Systems, St. Louis). A 4-kb *Ahr* partial digest *Bgl*II fragment downstream of exon 2 was subcloned into the *Bam*HI site of the plasmid pPNT (17), generating plasmid 314Bg4. A 10-kb *Mlu*I fragment upstream of exon 2 was subcloned into pSL1180 (Pharmacia Biosystems) and excised as a 7 kb *Sph*I fragment. This fragment was blunt-ended into the *Sma*I site of pBSK (Stratagene), excised with *Xho*I/*Not*I, and subcloned into the corresponding sites of 314Bg4, generating plasmid pPNTAhr2. The targeting construct contains 7 kb of homology upstream of the neomycin gene and 4 kb downstream.

Embryonic Stem (ES) Cell Culture. The CCE and R1 ES cell lines were grown on a feeder layer of mitomycin-C inactivated SNL fibroblasts under standard conditions with a 1:2500 dilution of conditioned media from the 720LIFD cell line (gift of Genetics Institute, Cambridge, MA) (18, 19). Linearized targeting DNA (30 μg) was mixed with 2×10^7 ES cells and electroporated with a Bio-Rad Gene Pulser at 250 V and 500 μF. Cells were subjected to selection in 200 μg of G418 per ml (GIBCO/BRL) and 1 μM Ganciclovir (Syntex, Palo Alto, CA). After 10 days, individual clones were expanded for freezing and genomic DNA isolation. Genomic DNA was prepared from ES cell clones and mouse tails by standard protocols and analyzed by Southern blot (20, 21).

Generation and Maintenance of Mice. Blastocysts were harvested from 3.5 day postcoital C57BL/6 females, microinjected with recombinant ES cells, and transferred into the uterine horns of 2.5-day postcoital pseudopregnant CD-1 females. Chimerism of the pups was scored by visual estimation of agouti coat color percentage. Male chimeras were backcrossed to C57BL/6 females and germline transmission assessed by agouti coat color in the resulting pups. Tail DNA from agouti pups was analyzed by Southern blot for the *Ahr* null allele. Mice were housed in microisolator cages in a specific-pathogen-free facility on aspen chip bedding (Sani-Chips) and fed autoclaved Purina Rodent Laboratory Diet 5010 ad libitum. Animals in the purified diet/bedding experiment were maintained on corncob bedding (Bed O'Cobs; Andersons) and fed AIN93G purified rodent diet (Dyets). For

Abbreviations: AHR, Ah receptor; *Ahr*, structural gene for the AHR; EROD, ethoxyresorufin O-deethylase; ES, embryonic stem; PAH, polycyclic aromatic hydrocarbon; TCDD, 2,3,7,8-tetrachlorodibenzo-*p*-dioxin.

¶To whom reprint requests should be addressed at: Department of Molecular Pharmacology and Biological Chemistry, Northwestern University Medical School, 303 East Chicago Avenue, Chicago, IL 60611. e-mail: c-bradfield@nwu.edu.

TCDD experiments 4- to 6-week old mice were injected i.p. with 7 μl TCDD in dioxane for a total dose of 3×10^{-8} mol/kg and control mice received an equivalent amount of dioxane.

Western Blot and Enzyme Analysis. Mouse livers were perfused with cold MENG buffer (25 mM MOPS/1 mM EDTA/0.02% NaN_3/10% glycerol, pH 7.5) containing 10 mM sodium molybdate and cytosolic and microsomal fractions were prepared. For Western blot analysis, 100 μg cytosolic protein (AHR) or 5 μg microsomal protein (P450s) was subjected to SDS/PAGE. Proteins were transferred to nitrocellulose and analyzed by Western blot as described (22). Two AHR polyclonal antibodies were used, a 1:500 dilution of G1295 and a 1:1000 dilution of BEAR-1 (22, 23). The mouse monoclonal AHR antibody VG9, which was generated against the C-terminal region of the human AHR and cross-reacts with the mouse AHR, was used at a 1:1000 dilution (W. Chan, personal communication). The cytochrome P450 antibodies were raised against rat P450s and obtained from Human Biologics (Phoenix, AZ); cytochrome P450 reductase and P450IIE1 antibodies were purchased from Daiichi Chemical Co. For the ethoxyresorufin O-deethylase (EROD) assay liver microsomal fractions were prepared 48 h after TCDD treatment and EROD activity was measured by a modification of the method of Pohl and Fouts (24). Values were normalized to microsomal protein concentration and a resorufin standard.

Histology. Tissues were fixed in 10% buffered formalin for 12 h and embedded in paraffin, and 4 μm sections were cut from equivalent regions for hematoxylin-eosin or trichrome staining. Interpretation of histology was independently performed by two pathologists who were blinded to specimen genotype.

RESULTS

Targeted Disruption of the *Ahr* Gene and Generation of *Ahr*$^{-/-}$ Mice. We used the positive–negative selection approach to disrupt the *Ahr* gene in ES cells (25). The *Ahr* targeting vector pPNTAhr2 was constructed in the plasmid pPNT (17) by using 129/Sv mouse genomic DNA (Fig. 1*A*). Our targeting vector was generated by replacing exon 2 with the neomycin resistance gene because this region encodes the basic/helix–loop–helix domain that is essential for dimerization and DNA binding (26). The R1 and CCE ES cell lines were electroporated with pPNTAhr2 and subjected to double selection with G418 and ganciclovir. Genomic DNA from doubly selected clones was analyzed by Southern blot with probe A (Fig. 1 *A* and *B*). This probe detects a 7-kb *Bam*HI restriction fragment in the wild-type ES cells. Construction of pPNTAhr2 replaced a 1-kb region surrounding exon 2 with the 2-kb neomycin cassette, resulting in a *Bam*HI fragment of 8 kb in homologous recombinant clones (Fig. 1 *A* and *B*). Screening of 525 ES cell clones yielded 15 homologous recombinants for a targeting frequency of 3%. Clones giving the correct pattern on Southern blot were probed with the neomycin gene. In all cases a single hybridizing band was found to comigrate with the recombined allele, indicating secondary integrations had not occurred (data not shown). Three CCE ES cell clones (C2, C50, and C121) and two R1 clones (R67 and R83) were microinjected into C57BL/6 blastocysts. Two CCE clones (C2 and C50) and both R1 clones gave rise to highly chimeric animals. Only the R67 clone contributed to the germline, yielding agouti pups upon backcross to C57BL/6 mice. *Ahr*$^{+/-}$ mice were interbred to generate *Ahr*$^{-/-}$ mice (Fig. 1*C*).

Disruption of the *Ahr* Gene Results in a Null Allele. Liver cytosols from *Ahr*$^{+/+}$, *Ahr*$^{+/-}$, and *Ahr*$^{-/-}$ mice were analyzed by Western blot for expression of the AHR protein. Three antibodies were used that recognized the N-terminal, PAS domain, and C-terminal regions of the AHR (G1295, BEAR-1, and VG9, respectively) (Fig. 2*A*). As a control for antibody specificity, we included liver cytosols from C57BL/6 and DBA/2 mice to display the mobilities of the AHR protein encoded by the *Ahr*$^{b\text{-}1}$ (97 kDa) and *Ahr*^{d} (104 kDa) alleles carried by C57BL/6 and 129/Sv mouse strains, respectively (Fig. 2*B*) (27). The expected 97-kDa AHR immunoreactive band was detected in the *Ahr*$^{+/+}$ animals that carry two C57BL/6 alleles (Fig. 2*B*). *Ahr*$^{+/-}$ mice show an ≈50% reduction in this 97-kDa protein band, indicating the presence of a single C57BL/6 *Ahr* allele and one inactivated 129/Sv allele. The *Ahr*$^{-/-}$ mice have no AHR protein detectable with any of the antibodies, confirming that they are homozygous for the inactivated 129/Sv *Ahr* allele. No smaller immunoreactive bands that might represent truncated or aberrant AHR protein were observed. Analysis of *Ahr*$^{+/+}$, *Ahr*$^{+/-}$, and *Ahr*$^{-/-}$ mouse liver RNA by reverse transcription–PCR indicated the presence of an mRNA transcript produced from the targeted allele. Cloning and sequencing of the amplification product indicated

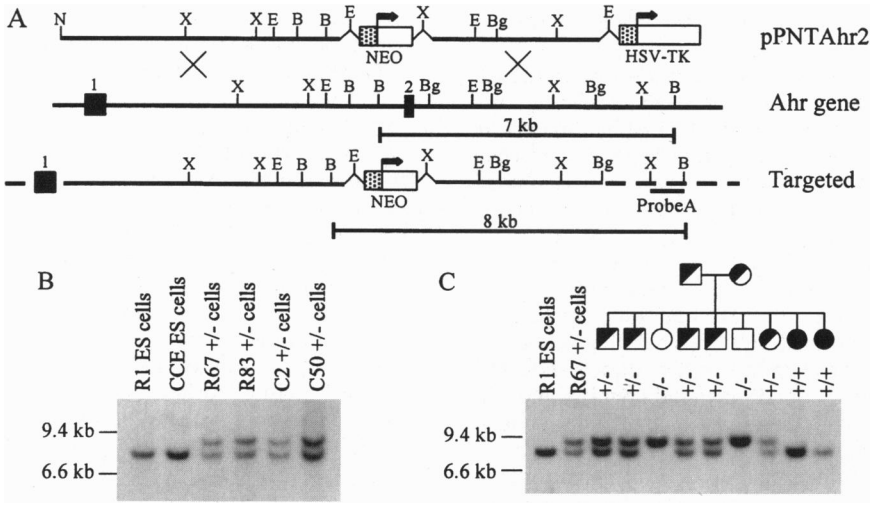

FIG. 1. Targeted disruption of the *Ahr* gene. (*A*) Schematic of the *Ahr* targeting construct pPNTAhr2 aligned with the homologous region of the *Ahr* structural gene and the structure of the recombinant allele. Black boxes denote exons, and probe A used to detect the recombinant allele is indicated. B, *Bam*HI; Bg, *Bgl*II; E, *Eco*RI; N, *Not*I; X, *Xba*I. (*B*) Southern blot analysis of parent and targeted ES cell clones. Parent R1 and CCE ES cells show only the wild-type 7-kb allele with probe A, while the targeted clones show a 7-kb wild-type and an 8-kb recombinant allele. (*C*) Southern blot analysis of tail DNA from offspring of an *Ahr*$^{+/-}$ mating. Solid symbols represent *Ahr*$^{+/+}$ mice, half-filled symbols represent *Ahr*$^{+/-}$ mice, and open symbols represent *Ahr*$^{-/-}$ mice; squares represent males and circles females.

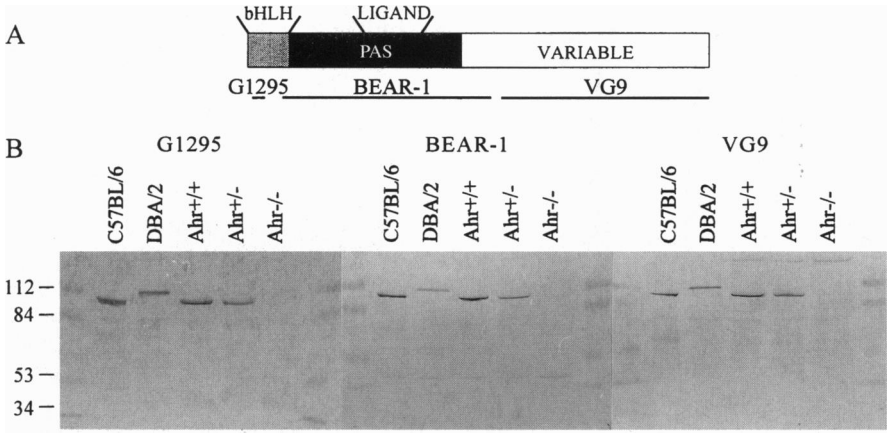

FIG. 2. The targeted *Ahr* allele produces no AHR protein. (*A*) Schematic of the AHR protein and the regions recognized by the antibodies G1295, BEAR-1, and VG9. (*B*) Western blots of mouse liver cytosol with the three AHR antibodies.

that exon 1 had been spliced to exon 3, generating a frame-shift and termination codon 7 residues past the splice junction (data not shown).

***Ahr*$^{-/-}$ Mice are Viable and Fertile.** At 2 weeks of age *Ahr*$^{+/+}$, *Ahr*$^{+/-}$, and *Ahr*$^{-/-}$ mice were found in the proportions 24%:52%:24% (159 mice), indicating no lethality associated with the null allele. *Ahr*$^{-/-}$ mice displayed a slower growth rate and decreased body weight compared to *Ahr*$^{+/+}$ mice for the first 3 weeks of life (data not shown). The *Ahr*$^{-/-}$ male and female mice were outbred to C57BL/6 animals, as well as inbred, and both males and females are fertile.

Cytochrome P450IA1 Is Not Induced in *Ahr*$^{-/-}$ Mice. As a measure of AHR function in *Ahr*$^{+/+}$, *Ahr*$^{+/-}$, and *Ahr*$^{-/-}$ mice, we determined the inductive response of cytochromes P450IA1 and P450IA2 to TCDD treatment. Induction was first measured enzymatically by determining the dealkylation rate of 7-ethoxyresorufin (EROD activity) in liver microsomal fractions, an enzymatic activity representative of both P450IA1 and P450IA2 isoforms (Fig. 3*A*). *Ahr*$^{+/+}$ mice displayed a small amount of EROD activity in the absence of TCDD, presumably the result of basal levels of P450IA2 (28). Upon TCDD treatment, EROD activity in *Ahr*$^{+/+}$ and *Ahr*$^{+/-}$ animals was induced ≈100-fold compared to vehicle controls. In contrast, *Ahr*$^{-/-}$ mice displayed a decreased basal level of EROD activity and were unresponsive to TCDD treatment. The individual induction profiles of P450IA1 and P450IA2 were further investigated by Western blotting with antisera specific for each isoform (Fig. 3*B*). Specific bands were observed for both isoforms in TCDD-treated *Ahr*$^{+/+}$ liver microsomal fractions. In *Ahr*$^{-/-}$ mice, however, cytochrome P450IA1 was undetectable, suggesting complete dependence on the AHR for expression of this enzyme. Cytochrome P450IA2 was also unresponsive to TCDD treatment in the *Ahr*$^{-/-}$ mice (Fig. 3*B*). Loading of increased amounts (10 μg) of microsomal protein revealed that *Ahr*$^{-/-}$ constitutive levels of P450IA2 were decreased to ≈25% of the *Ahr*$^{+/+}$ levels (data not shown). Therefore, cytochrome P450IA2 appears to be only partly dependent on the AHR for constitutive expression but entirely dependent for TCDD induction. As controls, antisera were also used to investigate the levels of related enzymes that are known to be unaffected by TCDD treatment—i.e., cytochrome P450 reductase and cytochrome P450IIE1. Analysis of *Ahr*$^{+/+}$, *Ahr*$^{+/-}$, and *Ahr*$^{-/-}$ mice indicated that these enzymes did not vary with either TCDD treatment or the *Ahr* genotype (data not shown).

***Ahr*$^{-/-}$ Mice Display a Complex Liver Phenotype.** All major organ systems of the *Ahr*$^{-/-}$ mice were examined macroscopically and microscopically. Tissues examined at 3 and 6 weeks were liver, lung, kidney, spleen, heart, brain, intestine, bladder, thymus, pancreas, skin, and ovary/uterus or testis. With the exception of liver at 3 and 6 weeks and some spleens at 6 weeks, all tissues appeared normal. When liver weights were expressed as percentage of body weight, *Ahr*$^{-/-}$ animals were found to have livers that were ≈25% smaller than their *Ahr*$^{+/+}$ littermates (Fig. 4). This difference in relative liver weight persisted even once total body weight normalized at 4 weeks. The livers of *Ahr*$^{+/-}$ animals were not different in size from the *Ahr*$^{+/+}$ mice at any time point examined.

Upon gross examination, the livers of 1 week old *Ahr*$^{-/-}$ mice revealed a pale and mottled appearance with a spongy texture (Fig. 5*A*). This phenotype was not apparent in newborn animals and in most cases had completely disappeared by 2 weeks of age. At all other ages examined, *Ahr*$^{-/-}$ livers appeared macroscopically normal although smaller. Histological analysis of 1-week-old *Ahr*$^{-/-}$ livers showed extensive microvesicular fatty metamorphosis of hepatocytes and prolonged extramedullary hematopoiesis compared to *Ahr*$^{+/+}$ littermates (Fig. 5 *B–E*). The fatty metamorphosis was patchy

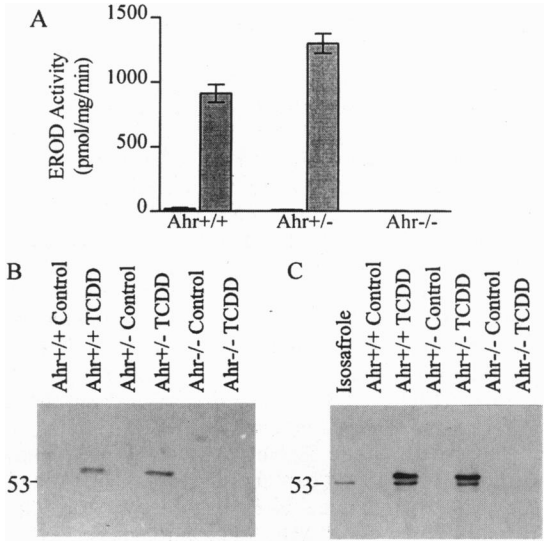

FIG. 3. Cytochrome P450IA1 and P450IA2 are not induced by TCDD in *Ahr*$^{-/-}$ mice. (*A*) EROD activity of mouse liver microsomal fractions after control or TCDD treatment. Error bars represent the high and low values obtained from two animals. (*B* and *C*) P450 Western blotting with specific antisera. *B* is with a monoclonal antibody specific for P450IA1 and *C* is with a polyclonal antibody recognizing both P450IA1 and P450IA2; the upper band represents P450IA1 and the lower P450IA2. The "isosafrole" lane contains microsomal protein from a mouse treated with this selective P450IA2 inducer.

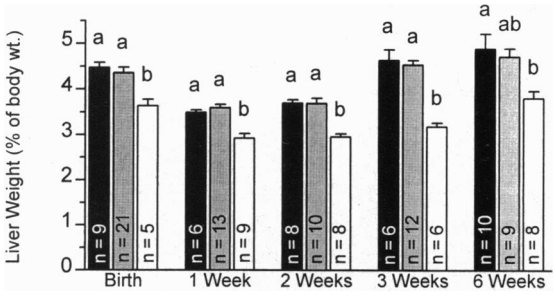

FIG. 4. $Ahr^{-/-}$ mice have smaller livers than $Ahr^{+/+}$ littermates. Liver weights were expressed as a percentage of body weight from birth through 6 weeks of age. Black bars represent $Ahr^{+/+}$ mice, gray bars $Ahr^{+/-}$ mice, and white bars $Ahr^{-/-}$ mice; the number of animals examined in each group is indicated within the bar. One-way ANOVA was performed using Tukey's multiple comparison procedure to identify the differences between groups ($P \leq 0.05$) and error bars represent SEM. For each time point those genotypes not sharing superscripts (a or b) are significantly different.

in all $Ahr^{-/-}$ livers but was not consistently pericentral or periportal. Both phenotypes showed a range of severity, but were present in all $Ahr^{-/-}$ animals; the extramedullary hematopoiesis was noted to be milder in those $Ahr^{-/-}$ mice with the most extensive fatty metamorphosis. By 3 weeks of age all evidence of fatty metamorphosis had disappeared and only small pockets of hematopoietic cells remained in the $Ahr^{-/-}$ livers. In addition, the majority of $Ahr^{-/-}$ mouse livers revealed mild to moderate hypercellularity with thickening and fibrosis in portal regions by 2 weeks of age (Fig. 5 *F* and *G*). The portal fibrosis was confirmed by using trichrome staining (Fig. 5 *H* and *I*).

Adult $Ahr^{-/-}$ Mice Exhibit Subtle Changes in Splenic Architecture and Mononuclear Cell Numbers. Although no statistically significant change in relative spleen weights in $Ahr^{-/-}$ mice was found, we observed that ≈50% of 6-week-old $Ahr^{-/-}$ animals exhibited enlarged spleens compared to $Ahr^{+/+}$ mice (Fig. 6*A*). The histologic appearance of the enlarged spleens was suggestive of congestive splenomegaly, with an increased erythroid component and smaller germinal centers (data not shown). To determine if this increase in spleen size was associated with alterations in the lymphoid population, we investigated the number of total splenic mononuclear cells in mice from 2 through 6 weeks of age. $Ahr^{+/+}$, $Ahr^{+/-}$ and $Ahr^{-/-}$ mice showed no differences in splenic mononuclear cell numbers at 2 or 3 weeks of age; however, at 6 weeks an ≈50% increase was seen in the $Ahr^{-/-}$ animals (Fig. 6*B*). Flow cytometry was used to assess the ratios of individual immune cell populations in 3- and 6-week-old $Ahr^{-/-}$ mice (data not shown). Analysis of spleen, thymus, and lymph node cell populations showed no differences in B lymphocytes (IgM and B220 staining) or T lymphocytes (CD3, CD4, and CD8 staining) in $Ahr^{+/+}$ versus $Ahr^{-/-}$ mice. Furthermore, myeloid populations (CD11b, CD18, and GR-1 staining) in the spleen and bone marrow were unchanged.

The $Ahr^{-/-}$ Phenotype Is Not Altered by Environmental Modulation. One possible explanation for the hepatic phenotype seen in $Ahr^{-/-}$ mice is liver toxicity resulting from background amounts of PAHs that cannot be appropriately biotransformed and excreted due to the lack of an AHR-mediated metabolic response. It has been demonstrated that mice maintained on standard laboratory chow and wood chip bedding will display some receptor-mediated responses, presumably due to the presence of trace PAH contaminants with agonist activity. Maintenance of laboratory mice on corncob bedding and a purified synthetic rodent diet has been shown to remove nearly all exogenous P450 inducers (29–31). To test the idea that $Ahr^{-/-}$ mice might be unable to mediate the enzymatic elimination of compounds present in their environment,

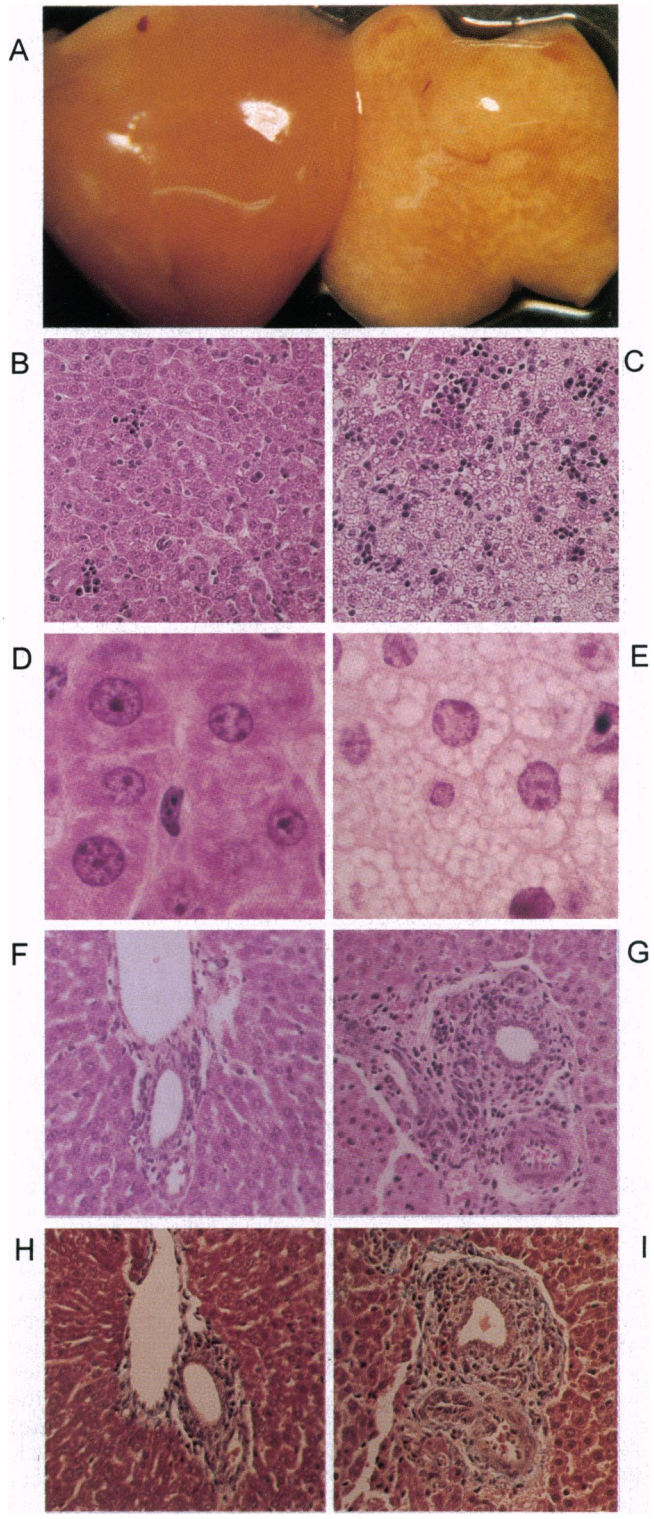

FIG. 5. Macroscopic and microscopic appearance of mouse livers. (A) Macroscopic appearance of livers from 1-week-old $Ahr^{+/+}$ (all at *Left*) and $Ahr^{-/-}$ (all at *Right*) mice. (*B* and *C*) Hematoxylin-eosin stained sections of livers from 1-week-old $Ahr^{+/+}$ and $Ahr^{-/-}$ mice demonstrating extensive microvesicular fatty metamorphosis and extramedullary hematopoiesis in the $Ahr^{-/-}$ animals. (*D* and *E*) Higher power view of 1-week-old $Ahr^{+/+}$ and $Ahr^{-/-}$ livers. (*F* and *G*) Hematoxylin-eosin stained liver sections from 2-week-old $Ahr^{+/+}$ and $Ahr^{-/-}$ mice demonstrating hypercellularity and fibrosis of the portal tract in the $Ahr^{-/-}$ animal. (*H* and *I*) Trichrome staining for connective tissue highlighting the portal fibrosis in $Ahr^{-/-}$ versus $Ahr^{+/+}$ mouse liver.

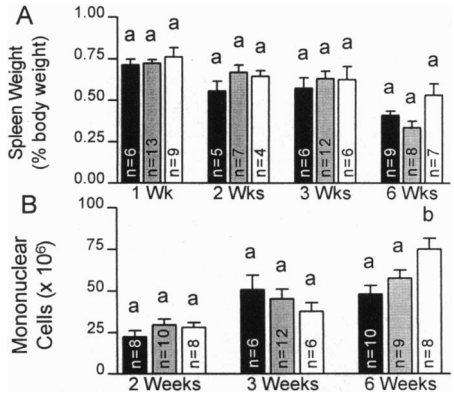

FIG. 6. Six-week-old $Ahr^{-/-}$ mice exhibit increased splenic mononuclear cells. (*A*) Spleen weights expressed as a percentage of body weight from 1–6 weeks of age. (*B*) Total splenic mononuclear cell counts from 2–6 weeks of age. Mononuclear cell suspensions were prepared from spleens and trypan blue excluding cells were counted in a hemacytometer. Black bars represent $Ahr^{+/+}$ mice, gray bars $Ahr^{+/-}$ mice and white bars $Ahr^{-/-}$ mice; the number of animals examined in each group is indicated within the bar. One-way ANOVA was performed using Tukey's multiple comparison procedure to identify the differences between groups ($P \leq 0.05$) and error bars represent SEM. For each time point those genotypes not sharing superscripts (a or b) are significantly different.

we housed $Ahr^{+/-}$ breeding pairs on a purified synthetic diet and corncob bedding for several weeks prior to mating and following the birth of their offspring. When the resulting $Ahr^{-/-}$ pups were analyzed at 1 and 2 weeks of age, they were found to have smaller livers and fatty metamorphosis to the same degree as $Ahr^{-/-}$ pups in a "standard" environment (Fig. 7 and data not shown).

DISCUSSION

In the initial analysis of our $Ahr^{-/-}$ phenotype, we focused on development from birth to 6 weeks. The $Ahr^{-/-}$ mice showed no increase in mortality, and at all ages examined exhibited ≈25% smaller livers than their $Ahr^{+/+}$ littermates. Two distinctive liver phenotypes were observed in the $Ahr^{-/-}$ mice between birth and 2 weeks of age. The most obvious phenotype, apparent at 1 week of age, was a macroscopically pale and spongy liver. Histological analysis revealed extensive microvesicular fatty metamorphosis, suggestive of a metabolic deficit in hepatocyte function. Second, we observed that $Ahr^{-/-}$ mice have a prolonged period of hepatic extramedullary hematopoiesis. The fatty metamorphosis resolves by 2 weeks of age and the extramedullary hematopoiesis by 3 weeks, suggesting a temporal requirement for the AHR in processes underlying these effects. At 2–3 weeks of age the majority of $Ahr^{-/-}$ mice

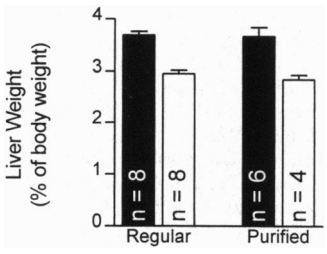

FIG. 7. Environmental modulation does not rescue the $Ahr^{-/-}$ phenotype. Liver weights expressed as a percentage of body weight for 2-week-old $Ahr^{-/-}$ offspring of $Ahr^{+/-}$ parents maintained in a standard environment or on a purified diet and corncob bedding. Black bars represent $Ahr^{+/+}$ mice and white bars represent $Ahr^{-/-}$ mice; the number of animals examined in each group is indicated within the bar.

begin to exhibit portal fibrosis and hypercellularity. It is presently unclear if the reduced liver size or the transient 1-week effects are causally related to this portal fibrosis. Although not statistically significant, approximately half of the 6-week-old $Ahr^{-/-}$ animals analyzed exhibited enlarged spleens with a histologic appearance suggestive of congestive splenomegaly, possibly resulting from sustained portal hypertension due to decreased liver blood flow (32).

The hepatic phenotype of our $Ahr^{-/-}$ animals could result from either an inherent defect in liver growth and metabolic maturation or a susceptibility to an unknown toxicant that causes hepatic abnormalities. Since we have eliminated many of the known environmental AHR agonists through the use of specialized diet and bedding, our data suggest that the $Ahr^{-/-}$ mice display a phenotype resulting from the loss of an AHR function unrelated to foreign compound exposure. Some precedent exists for the involvement of the AHR in processes related to the distinctive phenotypes we have observed. For example, reports have described extramedullary hematopoiesis and perturbations of hepatic lipid metabolism upon exposure to TCDD (11, 33). While a loss of the AHR should not be expected to mimic the effects of AHR activation by TCDD, these data suggest that the AHR may play a role in hepatic hematopoiesis or lipid metabolism. Although gene targeting experiments resulting in fatty liver have been rare, a recent report of the disruption of the cystathionine β-synthase gene described a hepatic phenotype with similarities to that seen in our $Ahr^{-/-}$ mice (34). $Cbs^{-/-}$ mice at 2–3 weeks of age have livers that appear light tan in color and microscopically show microvesicular fatty metamorphosis and extramedullary hematopoiesis. In contrast to $Ahr^{-/-}$ mice however, the $Cbs^{-/-}$ mouse livers are enlarged and the histologic pathology does not appear to resolve with time.

The results we have described here differ significantly from those of another group that has recently characterized a distinct *Ahr* mutation (35). These investigators generated an exon 1 *Ahr* deletion and thus for clarity we will designate their null allele $Ahr^{\Delta 1/\Delta 1}$ and our allele $Ahr^{\Delta 2/\Delta 2}$. The $Ahr^{\Delta 1/\Delta 1}$ mice display a spectrum of effects that were not observed in the $Ahr^{\Delta 2/\Delta 2}$ animals including 40–50% neonatal lethality with lymphocyte infiltration of lung, intestine, and urinary tract and an 80% reduction in splenic mononuclear cell numbers at 2 weeks of age. We observed no neonatal lethality in $Ahr^{\Delta 2/\Delta 2}$ mice maintained in separate colonies at Northwestern University and the University of Chicago. Additionally, we can find no evidence of immune cell decrease in our mice at 2–6 weeks of age. In fact, 6-week-old $Ahr^{\Delta 2/\Delta 2}$ mice appear to have a somewhat increased number of splenic mononuclear cells. Finally, histological examination of $Ahr^{\Delta 2/\Delta 2}$ mice at 1 week of age revealed no lymphocyte infiltration of major organs (data not shown). We also observed that $Ahr^{\Delta 2/\Delta 2}$ mice have a number of hepatic phenotypes not observed in $Ahr^{\Delta 1/\Delta 1}$ mice, such as a transient microvesicular fatty change accompanied by persistence of extramedullary hematopoiesis. Despite these differences, some important similarities were noted, since both $Ahr^{-/-}$ alleles are associated with decreased liver weights (although liver weight was reduced by 50% in $Ahr^{\Delta 1/\Delta 1}$ mice and only 25% in $Ahr^{\Delta 2/\Delta 2}$ mice), liver pathology, resistance to the inductive effects of TCDD, and decreased constitutive expression of cytochrome P450IA2. Recently, questions have been raised concerning the degree of portal fibrosis present in $Ahr^{\Delta 1/\Delta 1}$ mice (36). Our results suggest that portal hypercellularity and mild fibrosis is present in $Ahr^{\Delta 2/\Delta 2}$ mice, however this is in contrast to the more severe portal, and perhaps parenchymal, fibrosis described in $Ahr^{\Delta 1/\Delta 1}$ mice.

The reason for the differences in the two $Ahr^{-/-}$ mouse lines remains unclear. Targeted mouse lines generated by different groups that display phenotypic differences have been reported previously, as in the case of the gene encoding hepatocyte growth factor (37, 38). To explain differences at the *Ahr* locus,

we have considered possibilities such as genetic background effects, partial allelic inactivation, creation of alleles encoding proteins with new activities and differences in environmental factors. Since both $Ahr^{-/-}$ mouse lines were generated on 129 × C57BL/6 backgrounds, differences in genetic background are an unlikely cause. The possibility that the phenotypic differences result from a partial knockout in one of the mouse lines deserves further consideration from both groups. We initially addressed the possibility of a partial null allele by designing a targeting construct that deleted an essential domain and should preclude generation of functional protein through alternate splicing. Consistent with this design, we have shown that an incomplete deletion or formation of a novel protein is unlikely to have occurred from this targeted allele, since we detect no protein by Western blot. Analysis of AHR message or protein in the $Ahr^{\Delta 1/\Delta 1}$ mice was not included in their report; therefore it is unclear whether such an explanation warrants further consideration for that allele. A third possibility is that both mouse lines represent true null alleles, with differences resulting from environmental factors. Two experiments argue against such differences. Both modification of animal environment, by the use of highly purified food and bedding material, and maintenance of the $Ahr^{\Delta 2/\Delta 2}$ colony in multiple animal facilities had no effect on the pathology noted above. Thus, clarification of the differences between these two mouse lines may require intercrossing and direct comparisons within the same environment; such experiments would be beneficial once $Ahr^{\Delta 1/\Delta 1}$ mice become available. Interestingly, a second locus involved in xenobiotic metabolism has been inactivated by two groups with conflicting results (39, 40). The phenotype of mice deficient in P450IA2 has been variably described as being lethal at birth due to respiratory distress, or as being fully viable with no deficiencies other than in P450IA2-mediated drug metabolism.

The initial motivation for this work was to develop a model system to characterize AHR-independent effects of environmental toxicants. Given the phenotype we have described, however, such experiments should not be initiated hastily. The subtle liver deficits observed in $Ahr^{-/-}$ mice limit their usefulness in toxicological studies due the unavailability of control animals with a normal AHR but similarly compromised liver function. $Ahr^{-/-}$ mice are also likely to display markedly different disposition of hydrophobic planar aromatic compounds, a second phenomenon that will be difficult to control in toxicology studies. While we attempt to solve these problems, however, the $Ahr^{-/-}$ mice will allow us to tackle a more fundamental question as we attempt to understand the role that the AHR plays in normal liver growth and development.

We thank Andras Nagy (University of Toronto) for the R1 cells, Henry Pitot (University of Wisconsin) for interpretation of histology, Alan Poland (University of Wisconsin) for the BEAR-1 antibody, Sanjay Jain for numerous discussions, and Cynthia Clendenin, Catherine Rucker and Kirsten Sigrist for technical assistance. This work was supported by grants from the National Institutes of Health (ES06883 to C.A.B., HL52094-01 to M.C.S., and Predoctoral Training Grant CA09560 to J.V.S.) and the Pew Foundation. M.C.S. in an investigator of the Howard Hughes Medical Institute.

1. Burbach, K. M., Poland, A. & Bradfield, C. A. (1992) *Proc. Natl. Acad. Sci. USA* **89,** 8185–8189.
2. Ema, M., Sogawa, K., Watanabe, N., Chujoh, Y., Matsushita, N., Gotoh, O., Funae, Y. & Fujii-Kuriyama, Y. (1992) *Biochem. Biophys. Res. Commun.* **184,** 246–253.
3. Jones, P. B. C., Galeazzi, D. R., Fisher, J. M. & Whitlock, J. P., Jr. (1985) *Science* **277,** 1499–1402.
4. Gonzalez, F. J., Tukey, R. H. & Nebert, D. W. (1984) *Mol. Pharmacol.* **26,** 117–121.
5. Sutter, T. R., Tang, Y. M., Hayes, C. L., Wo, Y.-Y. P., Jabs, E. W., Li, X., Yin, H., Cody, C. W. & Greenlee, W. F. (1994) *J. Biol. Chem.* **269,** 13092–13099.
6. Telakowski-Hopkins, C. A., King, R. G. & Pickett, C. B. (1988) *Proc. Natl. Acad. Sci. USA* **85,** 1000–1004.
7. Favreau, L. V. & Pickett, C. B. (1991) *J. Biol. Chem.* **266,** 4556–4561.
8. Lamb, J. G., Straub, P. & Tukey, R. H. (1994) *Biochemistry* **33,** 10513–10520.
9. Whitlock, J. P. (1987) *Pharmacol. Rev.* **39,** 147–161.
10. Pitot, H. C., Goldsworthy, T., Campbell, H. A. & Poland, A. (1980) *Cancer Res.* **40,** 3616–3620.
11. Poland, A. & Knutson, J. C. (1982) *Annu. Rev. Pharmacol. Toxicol.* **22,** 517–554.
12. Bradfield, C. A., Kende, A. S. & Poland, A. (1988) *Mol. Pharmacol.* **34,** 229–237.
13. Perdew, G. H. (1988) *J. Biol. Chem.* **263,** 13802–13805.
14. Wilhelmsson, A., Cuthill, S., Denis, M., Wikstrom, A. C., Gustafsson, J. A. & Poellinger, L. (1990) *EMBO J.* **9,** 69–76.
15. Hoffman, E. C., Reyes, H., Chu, F. F., Sander, F., Conley, L. H., Brooks, B. A. & Hankinson, O. (1991) *Science* **252,** 954–958.
16. Reyes, H., Reisz-Porszasz, S. & Hankinson, O. (1992) *Science* **256,** 1193–1195.
17. Tybulewicz, V. L. J., Crawford, C. E., Jackson, P. K., Bronson, R. T. & Mulligan, R. C. (1991) *Cell* **65,** 1153–1163.
18. Robertson, E., Bradley, A., Kuehn, M. & Evans, M. (1986) *Nature (London)* **323,** 445–448.
19. Nagy, A., Rossant, J., Nagy, R., Abramow-Newerly, W. & Roder, J. C. (1993) *Proc. Natl. Acad. Sci. USA* **90,** 8424–8428.
20. Ausubel, F. M., Brent, R., Kingston, R. E., Moore, D. D., Seidman, J. G., Smith, J. A. & Struhl, K. (1990) *Current Protocols in Molecular Biology* (Greene/Wiley-Interscience, New York).
21. Southern, E. M. (1975) *J. Mol. Biol.* **98,** 503–517.
22. Chan, W. K., Chu, R., Jain, S., Reddy, J. K. & Bradfield, C. A. (1994) *J. Biol. Chem.* **269,** 26464–26471.
23. Pollenz, R. S., Sattler, C. A. & Poland, A. (1994) *Mol. Pharmacol.* **45,** 428–438.
24. Pohl, R. J. & Fouts, J. R. (1980) *Anal. Biochem.* **107,** 150–155.
25. Mansour, S. L., Thomas, K. R. & Capecchi, M. R. (1988) *Nature (London)* **336,** 348–352.
26. Dolwick, K. M., Swanson, H. I. & Bradfield, C. A. (1993) *Proc. Natl. Acad. Sci. USA* **90,** 8566–8570.
27. Poland, A. & Glover, E. (1990) *Mol. Pharmacol.* **38,** 306–312.
28. Quattrochi, L. C., Vu, T. & Tukey, R. H. (1994) *J. Biol. Chem.* **269,** 6949–6954.
29. Brown, R. R., Miller, J. A. & Miller, E. C. (1954) *J. Biol. Chem.* **209,** 211–222.
30. Torronen, R., Pelkonen, K. & Karenlampi, S. (1989) *Life Sci.* **45,** 559–565.
31. Bradfield, C. A., Chang, Y. & Bjeldanes, L. F. (1985) *Food Chem. Toxicol.* **23,** 899–904.
32. Bowdler, A. J. (1983) *Clin. Haematol.* **12,** 467–488.
33. MacKenzie, S. A., Thomas, T., Umbreit, T. H. & Gallo, M. A. (1992) *Toxicol. Appl. Pharmacol.* **116,** 101–109.
34. Watanabe, M., Osada, J., Aratani, Y., Kluckman, K., Reddick, R., Malinow, M. R. & Maeda, N. (1995) *Proc. Natl. Acad. Sci. USA* **92,** 1585–1589.
35. Fernandez-Salguero, P., Pineau, T., Hilbert, D. M., McPhail, T., Lee, S. S. T., Kimura, S., Nebert, D., Rudikoff, S., Ward, J. M. & Gonzalez, F. J. (1995) *Science* **268,** 722–726.
36. McDonnell, W. M., Chensue, S. W., Askari, F. K., Moseley, R. H., Fernandez-Salguero, P., Gonzalez, F. J. & Ward, J. M. (1996) *Science* **271,** 223–224.
37. Schmidt, C., Bladt, F., Goedecke, S., Brinkmann, V., Zschiesche, W., Sharpe, M., Gherardi, E. & Birchmeier, C. (1995) *Nature (London)* **373,** 699–702.
38. Uehara, Y., Minowa, O., Mori, C., Shiota, K., Kuno, J., Noda, T. & Kitamura, N. (1995) *Nature (London)* **373,** 702–705.
39. Pineau, T., Fernandez-Salguero, P., Lee, S. S., McPhail, T., Ward, J. M. & Gonzalez, F. J. (1995) *Proc. Natl. Acad. Sci. USA* **92,** 5134–5138.
40. Liang, H.-C. L., Li, H., McKinnon, R. A., Duffy, J. J., Potter, S. S., Puga, A. & Nebert, D. W. (1996) *Proc. Natl. Acad. Sci. USA* **93,** 1671–1676.